RSC Advances

ROYAL SOCIETY OF CHEMISTRY

www.rsc.org/advances

	Nanchang, China Yu, Yanrong; Institute of immunotherapy and College of Basic Medicine of Nanchang University, and Jiangxi Academy of Medical Sciences, Nanchang, China; Jiangxi Provincial Key Laboratory of Immunotherapy, Nanchang, China Shi, Xiaofa; Institute of immunotherapy and College of Basic Medicine of Nanchang University, and Jiangxi Academy of Medical Sciences, Nanchang, China Fu, Yingyuan; Institute of immunotherapy and College of Basic Medicine of Nanchang University, and Jiangxi Academy of Medical Sciences, Nanchang, China Yuan, Ken; Institute of immunotherapy and College of Basic Medicine of Nanchang University, and Jiangxi Academy of Medical Sciences, Nanchang, China; Jiangxi Provincial Key Laboratory of Immunotherapy, Nanchang, China Zhou, Nanjin; Institute of immunotherapy and College of Basic Medicine of Nanchang University, and Jiangxi Academy of Medical Sciences, Nanchang, China; Jiangxi Provincial Key Laboratory of Immunotherapy, Nanchang, China Min, Weiping; Institute of immunotherapy and College of Basic Medicine of Nanchang University, and Jiangxi Academy of Medical Sciences, Nanchang, China; Jiangxi Provincial Key Laboratory of Immunotherapy, Nanchang, China

Subject area & keyword:	Biomedical < Biological

Synergic therapy of melanoma using GNRs-MUA-PEI/siIDO2-FA through targeted gene silencing and plasmonic photothermia

Yujuan Zhang[1,2*], Na Song[1,2], Jiamin Fu[1,2], Yanling Liu[1,2], Xuelin Zhan[1,2], Shanshan Peng[1,2], Zhi Yang[1,2], Xianfang Zhu[3], Yiguo Chen[1,2], Zhigang Wang[1,2], Yanrong Yu[1,2], Qiaofa Shi[1], Yingyuan Fu[1], Keng Yuan[1,2], Nanjin Zhou[1,2], Thomas E Ichim[4], Weiping Min[1,2,5*]

1. Institute of immunotherapy and College of Basic Medicine of Nanchang University, and Jiangxi Academy of Medical Sciences, Nanchang, China
2. Jiangxi Provincial Key Laboratory of Immunotherapy, Nanchang, China
3. China-Australia Joint Laboratory for Functional Nanomaterials, School of Physics and Mechanical and Electrical Engineering, Xiamen University, Xiamen, China
4. Batu Biologics Inc, San Diego, California, USA
5. Department of Surgery, Pathology and Oncology, University of Western Ontario, London, Canada

*** Correspondence to**: Drs. Yujuan Zhang (email: yujuanzhang@ncu.edu.cn) or Weiping Min (email: mweiping@uwo.ca).

Abbreviations: GNA, gold nanorods; FA, folic acid; IDO2, Indoleamine dioxygenase 2; PTT, photothermal therapy; TEM, transmission electron microscope; CTAB, cetyltrimethylammonium bromide; MUA, mercaptoundecanoic acid; PEI, Poly ethylene imine; siRNA, small interfering RNA; LSPR, localized surface plasmon resonance; LIP2000, lipofactamine 2000.

Abstract:
Indoleamine dioxygenase 2 (IDO2) is a newly discovered enzyme that contributes to tumor immune escape. Our previous studies demonstrated that small interfering RNA (siRNA)-mediated IDO2 knock-down induces tumor cell apoptosis and inhibits tumor growth. Modified gold nanorods (GNRs) are excellent siRNA nano-carriers as well as photothermal therapy agents, with potential to augment siRNA efficacy and target specificity. In this study, we developed a novel nanostructure of GNRs-MUA-PEI/siIDO2-FA for targeted therapy of melanoma. Firstly, we demonstrated that these new nanostructures possess excellent biocompatibility, as well as efficiently and specifically deliver RNA to melanoma cells. Secondly, IDO2 knockdown significantly enhanced the photothermal therapeutic efficacy of GNRs as evidenced by inducing increased tumor cell apoptosis *in vitro* as well as inhibiting the growth of tumors *in vivo* under low laser power density. Finally, we firstly demonstrated that GNRs-MUA-PEI/siIDO2-FA exerts synergistic effects on photothermal therapy and gene silencing IDO2 in anti-tumor therapy of inhibiting tumor growth, which holds great promise for anti-cancer therapeutics as an alternative strategy for the treatment of melanoma.

Keywords: Gold nanorods, Folic acid, IDO2, siRNA, melanoma, photothermal therapy

1. Introduction:

Metastatic melanoma is one of the most aggressive and lethal malignancies.[1] In the last decades, its global incidence has increased faster than for any other solid tumor with 160,000 new cases per year and 48,000 deaths.[2, 3] The conventional chemotherapy treatment of metastatic melanoma is using dacarbazine, but the response rate is low at only 15-20 %.[4] Immunotherapy has also been applied for metastatic melanoma therapy, which employs cytokines that stimulate the patient's immune system to fight cancer, such as interleukin-2 (IL-2), but high-dose IL-2 also has a low response rate of only 16%.[5]

Cancer immunotherapy is based on the recognition of tumor-associated antigens (peptides) on cancer cells by the patient's T cells. The US Food and Drug Administration (FDA)-approved immunotherapies such as IL-2, interferon (IFN)-α, anti-CTLA-4 (cytotoxic T lymphocyte antigen-4) and anti-PD-L1 (programmed death-ligand) all appear to activate and/or expand tumor-specific T cells of antigen specificity. This process requires the delivery of appropriate signals that initiate immune responses from being ineffective to being capable of rejecting established tumors.[6] One of the limiting factors of successful cancer immunotherapy is direct and indirect suppression of the immune response by the tumor, or by tumor-reprogrammed immune elements.[7-9] One of the major means of tumor mediated immune suppression is inhibition of T cell effector functions and generation of Treg by tryptophan catabolism due to the overexpression of tryptophan-degrading enzymes in human tumors and tumor associated macrophages, such as indoleamine-2,3-dioxygenase (IDOs) including IDO1 and IDO2. These enzymes are intracellular heme-containing enzymes that initiate the first and rate-limiting step of tryptophan degradation along the kynurenine pathway.[10, 11] We and others have demonstrated that RNAi-mediated suppression of IDOs enhances anti-tumor immunity in a variety of preclinical systems.[12-14] In addition to IDOs playing a role in immune suppression, our recent studies revealed that IDO2 may play a role in promotion of tumor cell viability in that knocking down expression of this enzyme resulted in enhanced apoptosis, chemosensitivity, and reduced tumor growth in the B16-BL6 model of metastatic melanoma.[15, 16]

Ever since RNA interference (RNAi) was discovered, this technology has emerged as a promising treatment strategy for cancer, which could effectively knockdown or silence target genes.[17] However, small interfering RNA (siRNA) is unstable in the blood stream, and are unable to penetrate cell membranes, in part due to their large size and negative charge.[18] Successful application of siRNA for cancer therapy is highly dependent on the development of delivery vehicles that are nontoxic and enable the selective and efficient transport of siRNA to a specific tissue.

Utilization of nanoparticles for targeting neoplastic tissue has been successfully performed since 1995.[19] Physical features of nanoparticles such as size and shape play a critical role in overall tissue permeability, as well as selectivity of delivery to malignant versus non-malignant tissue. Additionally, the characteristics of the nanoparticles are

fundamental factors in determining pharmacokinetics and biodistribution.[20] A limited number of nanoparticle systems have been developed that were successful in crossing the threshold to clinical entry. [21] Various shapes of nanoparticles have been developed in order to provide a higher level of control over pharmacokinetic and delivery parameters [22]. For example, cylindrical shaped nanoparticles possess enhanced ability to remain in systemic circulation as compared to spherical shapes. This is believed to be due to differences that the shapes cause on rigidity, surface area, and endothelial interactions. [23] In particular, cylindrical shapes are believed to be more advantageous for preclinical development by allowing passive accumulation in tumors and enhanced circulation time. [20]

Hyperthermia, the elevation of tumor temperature, is an established method used in cancer therapy.[24, 25] In cancer treatment, thermal therapies are mainly used for eliminating solid tumors. However, hurdles for clinical application of tumor hyperthermia exist due to limited ability to deliver sufficient heat in target regions without harming non-malignant tissue. More recently, studies have taken advantage of nanotechnology based approaches for enhancing specificity and efficacy of directed hyperthermia. One promising application of nanotechnology is utilization of light with a wavelength that matches oscillations of the conduction band electrons on gold nanorods (GNRs). When this occurs, the surface plasmon resonance (SPR) on nanostructures is reached, which allows light to be absorbed and to be converted to heat; this approach is called photothermia or plasmonic photothermia.[26-28] When such nanoparticles are localized within tissue with the intention of using this technique as a tool to induce hyperthermia, it is termed photothermal therapy (PTT) or plasmonic photothermal therapy (PPTT).[27, 28] With PPTT, many groups have achieved tumor selective temperatures from 50 ^{o}C to over 70 ^{o}C which are well above the threshold required for vascular damage and cell death.[27, 29-31] Thus, specific delivery of GNRs is highly desirable in clinical PPTT.

In the present work, we firstly developed a novel nanostructure, GNRs-MUA-PEI/siIDO2-FA, which consists triple advantages: 1) a folic acid (FA) adaptor specifically targeting tumor cells; 2) GNRs inducing robust tumor killing in photothermal therapy; and 3) siIDO2 specifically silencing IDO2 to induce tumor cell apoptosis. We established a two-step method to prepare a novel siRNA nanocarrier of GNRs-MUA-PEI-FA that was composed of folic acid-coated gold nanorods and siIDO2. This structure not only displayed high siRNA loading capacity and low cytotoxicity, but also facilitated the tumor-specific targeting to B16-BL6 cells. Additionally, siRNA delivered by GNRs-MUA-PEI/siIDO2-FA could silence IDO2 effectively, while IDO2 knockdown enhanced apoptosis of B16-BL6 cells *in vitro* and *in vivo*. Moreover, we demonstrated the clinical potential of PTT using GNRs-MUA-PEI/siIDO2-FA, as evidenced by the remarkable suppression of tumor growth in a murine melanoma model. This novel nanoplatform GNRs-MUA-PEI/siIDO2-FA exerts synergistic effects of tumor-targeted photothermal therapy and IDO2 gene silencing on suppressing tumor growth, which could be as an

alternative new strategy of PTT for treating melanoma and holds great promise for anti-cancer therapeutics.

2. Materials and Methods

2.1. Synthesis of GNRs.

Water-soluble gold nanorods were synthesized via seed-mediated growth routes as previously described.[32] Briefly, first a seed solution was prepared as follows: 1 mL of cetyltrimethylammonium bromide (CTAB) solution (0.2 M) was mixed with 1 mL of $HAuCl_4$ (0.5 mM). While the solution was stirred at 25 ^oC, 0.12 mL of ice-cold 0.01 M $NaBH_4$ was added, and the resulting seed solution turned to brownish yellow color. Secondly, the growth solution was prepared as follows: 50 mL of $HAuCl_4$ (1 mM), 50 mL of CTAB (0.2 M) and 2.5 mL of $AgNO_3$ (4 mM) were mixed at 25 ^oC, and after gentle mixing, 670 μL of ascorbic acid (0.079 M) was added, and then the color changed from dark yellow to colorless. To generate nanorods, 120 μL of the seed solution was added to the growth solution at 27-30 ^oC under gently mixing. Within 10-20 minutes, the combined solution gradually changed colors to brownish red. After 24 hours, the solution was then centrifuged at 12000 rpm for 15 minutes to remove the excessive CTAB. Finally, the nanorod sample coated with CTAB was characterized by Transmission electron microscope (TEM) and UV-vis-NIR spectrometer.

2.2. Synthesis of GNR-MUA-PEI and GNR-MUA-PEI-FA.

Synthesis of MUA-PEI and MUA-PEI-FA is based on the chemical reaction between amino group and carboxyl group. In brief, the steps were designed to covalent conjugate (1) carboxyl groups of MUA binding to amino groups of poly ethylene imine (PEI) by ethyl(dimethylaminopropyl) carbodiimide (EDC) mediated amidation with N-Hydroxysuccinimide (NHS) in $HCCl_3$, and (2) carboxyl groups of folic acid (FA) binding to residual amino groups of PEI by the similar reaction of EDC mediated amidation with NHS but in DMSO instead of in $HCCl_3$. MUA-PEI to replace CTAB on GNRs obtained the GNRs-MUA-PEI, and 1:1 ratio of MUA-PEI to MUA-PEI-FA to replace CTAB on GNRs obtained the GNRs-MUA-PEI-FA. The products were centrifuged and characterized by TEM, UV-vis-NIR spectrometer and Fourier Transform Infrared spectroscopy (FTIR).

2.3. siRNA synthesis.

The siRNAs targeting IDO2 mRNA or GAPDH were generated in accordance with the target sequence selection methods described by Jin et al.[33] siRNA was synthesized by the manufacturer (Sigma, St. Louis, MO). siRNA targeting luciferase gene GL2 (GL2 siRNA)

was used as a scrambled-silencing control since GL2 is not expressed in treated cells.

2.4. Synthesis of GNR-MUA-PEI/siRNA-FA and gel shift assays.

Equal volumes containing 0.5 μg of siRNA and the desired amount of GNR-MUA-PEI-FA (the weight ratios of siRNA to GNR-MUA-PEI-FA were 1:0, 1:1, 1:2, 1:3, 1:4, 1:5, 1:6, 1:7, 1:8) were mixed and incubated for 30 minutes. The resulting complexes were electrophoresed at 80 V using 1.5 % agarose gel and EtBr in TAE buffer. After 20 minutes, the gel was removed, visualized under UV lamp and the picture was taken with an Olympus C8080 digital camera.

2.5. Cell culture.

A murine melanoma cell line established from a C57BL/6 mouse and designated B16-BL6 was obtained from the American Type Culture Collection and was maintained in RPMI 1640 medium (Sigma-Aldrich) with 10 % FBS, L-glutamine, penicillin, and streptomycin at 37 ^{o}C in 5 % CO_2.

2.6. MTT assay.

MTT (3-(4,5-Dimethylthiazol-2-yl)-2,5-diphenyltetrazolium bromide) cytotoxicity assay. A MTT kit (BD Pharmingen, San Diego, CA) was required. B16-BL6 cells (6×10^3) were seeded in a 96 well microplate. After 24 hours, fresh medium containing GNR-CTAB or GNR-MUA-PEI-FA were added, and the final concentration of GNR-CTAB or GNR-MUA-PEI-FA was 20 μg/mL, 40 μg/mL, 60 μg/mL, 80 μg/mL, 100 μg/mL, 150 μg/mL, and 200 μg/mL. After 24 or 48 hours, the MTT reagent was added for another 4 hours and was converted by the mitochondrial reductase. The resulting purple crystals were dissolved in solubilization buffer and spectrophotometrically analyzed at 490 nm, using a reference of 650 nm in a microplate reader (SpectraMax M5e).

2.7. Apoptosis assay.

The apoptotic and necrotic cell distribution were determined by Annexic V-FITC/PI Apoptosis Detection Kit (BD Pharmingen, San Diego, CA). The B16-BL6 cells were plated in 12-well microplates at a density of 1×10^5 cells/well. After 24 hours incubation, the medium was replaced with fresh medium and a series amount of GNR-CTAB or GNR-MUA-PEI-FA were added to the medium and the final concentration of GNR-CTAB or GNR-MUA-PEI-FA was 20 μg/mL, 40 μg/mL, 60 μg/mL, 80 μg/mL, 100 μg/mL, 150 μg/mL, and 200 μg/mL. After 24 hours or 48 hours, the cells were trypsinized, harvested, washed with PBS and resuspended in 100 μL of binding buffer containing 1 μL Annexin V-FITC and 2 μL PI. After incubation at room temperature for 15 minutes in the dark, 100 uL of binding buffer was added to each sample before washing and then the samples were resuspended in medium and analyzed by BD FACS Calibur (BD Biosciences, Mountain

View, CA).

2.8. Cellular uptake.

The same amounts (1 μg) of Cy3-GAPDH were used to assess the cellular uptake of LIP2000 (Lipofectamine 2000, Invitrogen Life Technologies, as the positive control group), GNR-MUA-PEI and GNR-MUA-PEI-FA. Briefly, B16-BL6 or HUVEC cells were plated in 12-well microplates at a density of 1×10^5 cells/well. After 48 hours incubation, the medium was replaced with fresh medium, and then LIP2000/siRNA, GNR-MUA-PEI/siRNA (wt(GNR-MUA-PEI):wt(siRNA)=15:1) and GNR-MUA-PEI/siRNA-FA (wt(GNR-MUA-PEI-FA):wt(siRNA)=15:1; 10:1; 8:1) which had been prepared with the same amount siRNA (1 μg) were added into the fresh medium and incubated with cells at 37 ^{o}C for 4 hours. Then, the cells were trypsinized, harvested, washed three times with PBS to remove unloaded nanoparticles and resuspended in 200 μL of the medium and analyzed by BD FACS Calibur (BD Biosciences, Mountain View, CA).

2.9. Gene silencing and PCR.

B16-BL6 cells were seeded in a 12-well plate with a density of 1×10^5 cells/well. After 24 hours, a final concentration of 16 μg/mL of GNR-MUA-PEI/siRNA-FA (wt(GNR-MUA-PEI-FA):wt(siRNA)=15:1) was added into the cells for 24 hours transfection, and then cells were lysed (Trizol reagent, Invitrogen) and total RNA was isolated according to the manufacturer's instructions. 1 μg of total RNA was synthesized to cDNA by using reverse transcriptase (MmLV-RT, Invitrogen). The mRNA expressions of IDO2 in the samples were quantified with q-PCR using GAPDH as a reference. The following primers sets were used for PCR amplifications: GAPDH, 5'-TGATGACATCAAGAAGGTGGTGAA-3' (sense) and 5'-TCCTTGGAGGCCATGTAGGCCAT-3' (antisense); IDO2, 5'-GTGGGGCTGGTCTATGAAGGTG-3' (sense) and 5'-TGGTGGCAGCGGAGATAATGTA-3'(antisense). q-PCR reactions were performed in a Stratagene Mx3000P QPCR System (Agilent Technologies, Lexington, MA) using SYBR green PCR Master Mix (Life technologies) according to manufacture's protocol. Differences in gene expression were calculated by using the △Ct method.

2.10. Western blot.

5×10^5 B16-BL6 cells were seeded into a 6-well plate and grown overnight. The cells were transfected with a final concentration of 16 μg/mL of GNR-MUA-PEI/siRNA-FA (wt(GNR-MUA-PEI-FA):wt(siRNA)=15:1) loading IDO2 siRNA or GL2 siRNA for 24 hours. The cells were harvested, washed twice with ice-cold PBS, resuspended in protein lysis buffer with complete protein inhibitor (Roche Diagnostics) and then keep the container on ice for 30 minutes. Lysed cells were centrifuged at 15000 rpm for 20 minutes at 4 ^{o}C and

the supernatant were collected and stored at -80 ^{o}C for future use. Protein concentration was determined by Bio-Rad protein assay and 50 μg of each group cell lysate was separated on 12 % SDS-PAGE, transferred to nitrocellulose membrane (Bio-Rad), blocked with 5 % fat-free milk (Carnation) and 3 % BSA in TBS-T (0.25 % Tween 20), probed with a mouse anti-human IDO2 mAb that binds to both human and mouse IDO2 (Santa Cruz Biotechnology) and goat anti-mouse GAPDH Ab (Sigma-Aldrich) according to the manufacturer's instructions, and visualized by an ECL assay (Amersham Biosciences).

2.11. In vitro photothermal effect of GNR-MUA-PEI-FA.

B16-BL6 cells (6×10^3) were seeded in a 96 well microplate, and after 24 hours the cells were incubated with a final concentration of 15 μg/mL of GNR-MUA-PEI-FA or PBS (as the control group) for overnight. And then, the cells were irradiated at 2 W/cm^2 for various times (0, 0.5, 1, 2, 5, 10 minutes) or at 5 minutes for different power density (0 W/cm^2, 0.5 W/cm^2, 1 W/cm^2, 2 W/cm^2, 4 W/cm^2). After 24 hours, the MTT reagent was added for another 4 hours and was converted by the mitochondrial reductase. The resulting purple crystals were dissolved in solubilization buffer and spectrophotometrically analyzed at 490 nm, using a reference of 650 nm in a microplate reader (SpectraMax M5e).

2.12. Apoptosis of tumor cells induced by GNR-MUA-PEI/siIDO2-FA.

B16-BL6 cells were seeded in a 24-well plate with a density of 0.5×10^5 cells/well and after 24 h those cells were incubated with PBS (as the control group) or a final concentration of 16 μg/mL of GNR-MUA-PEI/siGL2-FA (wt(GNR-MUA-PEI-FA):wt(siRNA)=15:1) or 16 μg/mL of GNR-MUA-PEI/siIDO2-FA (wt(GNR-MUA-PEI-FA):wt(siRNA)=15:1) in double for overnight, and then one was irradiated at 2 W/cm^2 for 5 minutes after the incubation with PBS or 16 μg/mL of GNR-MUA-PEI/siGL2-FA or 16 μg/mL of GNR-MUA-PEI/siIDO2-FA. The apoptotic and necrotic cell distribution of all were determined at 24 hours by Annexin V-FITC/PI Apoptosis Detection Kit and analyzed by BD FACS Calibur (BD Biosciences, Mountain View, CA).

2.13. Animals and tumor model and H&E staining.

Female C57BL/6 mice, 6–8 weeks of age and weighting 18–23 g, were purchased from Changsha Laboratory Animal Co. Ltd., and housed in a SPF grade animal center. The use of all mice in this study complied with the Regulations for the Administration of Affairs Concerning Experimental Animals of China and the ethical approval of institutional Animal Care and Use Committee of Nanchang University, China. The mice were anesthetized by isoflurane and inoculated with 2×10^6 B16-BL6 cells suspension. In order to evaluate the inoculation of tumor models, hematoxylin and eosin (HE) staining was performed on paraffin-embedded sections. The prepared specimen was examined using a light microscope.

2.14. Topical siRNA delivery.

C57BL/6 mice were anaesthetized and shaved, and the melanoma tumors were inoculated. After two weeks, mice were anesthetized, and Cy3-siGAPDH, GNR-MUA-PEI/Cy3-siGAPDH (wt(GNR-MUA-PEI):wt(siRNA)=15:1) and GNR-MUA-PEI/Cy3-siGAPDH-FA (wt(GNR-MUA-PEI-FA):wt(siRNA)=15:1) (all containing 6 μg of siRNA) respectively mixing with glycerin (50 % in final solution v/v) and DMSO (10 % in final solution v/v) and nuclease free water were topically massaged on the skins above the inoculated tumors. After 4 hours, the mice were scarified and the tumors were collected. The tumors attached to a freezing stage using an optimal cutting temperature (OCT) compound (Triangle Biomedical Sciences, USA) were frozen and cut into 1 mm horizontal sections. Images were visualized with a fluorescence microscope (Olympus, Model BX 51, Japan).

2.15. In vivo Photothermal Effect of GNR-MUA-PEI/siIDO2-FA.

Melanoma bearing mice were generated by inoculating 2×10^6 B16-BL6 cells suspension. When the diameter of tumor was about 3 mm, PBS (as the control group) or GNR-MUA-PEI-FA (wt(GNR-MUA-PEI-FA):wt(siRNA)=15:1), siRNA (6 μg, siIDO2 or siScramble), glycerol (50 % in final solution v/v), DMSO (10 % in final solution v/v) were mixed and applied onto the tumors on day 6, 10, 14, 18 . 12 hours after each application of above mixture, a laser irradiation irradiation (1 w/cm^2, 2 minutes) was conducted. The tumor sizes of growth were measured with caliper. 20 days after tumor inoculation, the mice were sacrificed and tumors were collected. The tumor weights were measured with a 2-digit electronic balance and the images were taken with a camera.

2.16. Statistics.

Data were presented as mean ± SD. Student's t-test (2-tailed) was applied to determine differences between two means. For the comparison of multiple groups, one-way ANOVA test was used. For all statistical analyses, differences with p values <0.05 were considered significant.

3. Results and Discussions

3.1. Synthesis, modification and characterization of GNRs.

First, we synthesized CTAB-stabilized GNRs using an established seed-mediated growth methods.[32] The synthesized GNRs were characterized by the transmission electron microscope (TEM) image, which showed that GNRs have a mean length of 39.0 ± 3.5 nm and width of 10.0 ± 1.5 nm (Figure 1A). GNR-MUA-PEI-FA that is shown in Figure 1B is prepared by 1:1 ratio of MUA-PEI to MUA-PEI-FA replacing CTAB on GNRs by one step. PEI carrying positive charges could bind the negative-charged siRNA due to the electrostatic interaction. In order to improve the cellular uptake of GNRs, folic acid (FA) was conjugated to GNRs using the chemical reaction between amino group and carboxyl group due to overexpression of FA receptors on B16-BL6 cells. As shown in Figure 1C, a longitudinal SPR maximum for the original GNRs-CTAB was at around 750 nm, and the peak slightly red-shifted to 770 nm for GNR-MUA-PEI, followed by another red-shift to 790 nm for GNR-MUA-PEI-FA, which suggests MUA-PEI and MUA-PEI-FA have been successfully bound on GNRs. Figure 1D shows the FTIR spectra of GNR-MUA-PEI and GNR-MUA-PEI-FA. Both of them have the following absorption: the absorption band of -CO-NH- at 1631cm^{-1} which suggested the chemical binding between the carboxyl group of MUA or FA and the amino group of PEI. Comparing with the FTIR spectra of GNR-MUA-PEI, a new absorption band appeared for GNR-MUA-PEI-FA at 1611 cm^{-1} and 1511 cm^{-1} which belongs to the vibration of benzene ring from FA. These results further suggested that FA was successfully conjugated. In order to improve the melanoma targeting efficiency and siRNA loading capacity simultaneously, we prepared that the ratio of MUA-PEI to MUA-PEI-FA was 1:1 on the surface of GNRs.

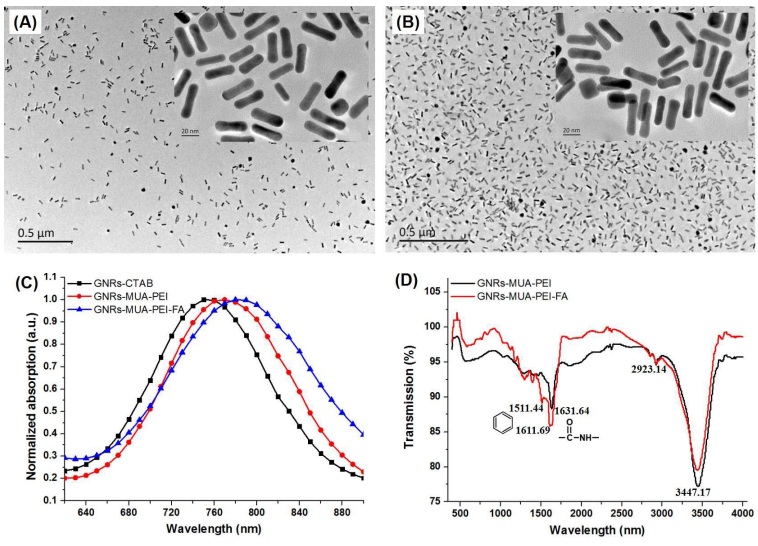

Figure 1. Characterization of GNRs. TEM images of (A) GNRs-CTAB and (B) GNRs-MUA-PEI-FA, (C) Normalized UV-Vis absorption spectra of GNRs-CTAB, GNRs-MUA-PEI and GNRs-MUA-PEI-FA, (D) FTIR

spectra of GNRs-MUA-PEI and GNRs-MUA-PEI-FA.

3.2. Attenuation of cytotoxicity of GNRs by FA

In this newly designed nanostructure, folic acid was not only used to bind the FA receptor on melanoma cells but also to attenuate the cytotoxicity of PEI. Next, we tested the cytotoxicity of the synthesized GNR-MUA-PEI-FA. As shown in Figure 2, after B16-BL6 cells were exposed to a series of GNR-CTAB and GNR-MUA-PEI-FA at various concentrations, we observed that B16-BL6 exposed to GNR-MUA-PEI-FA had higher cell viability than those in the presence of GNR-CTAB on the basis of MTT experiments. After incubation with GNR-CTAB (20 μg/mL) for 24 hours, the cytotoxicity was noticed (cell viability was decreased by 16.0 ± 5.91 %). The cytotoxicity was increased at higher concentrations: a dose of 100 μg/mL of GNR-CTAB reduced the cell viability by 50.5 ± 5.30 %; while the survival cells only left 16.3 ± 2.50 % when a higher concentration (200 μg/mL) of GNR-CTAB was added to B16-BL6 for 24 hours (Figure 2A). In contrast, a dose of 20 μg/mL of GNR-MUA-PEI-FA caused almost no drop on the cell viability, while even a high dose (200 μg/mL) just slightly decreased the cell viability about 30.5 ± 1.41 % (Figure 2A). The toxicity was significantly increased when extending the time of cell incubation even at very low concentration (20 μg/mL), the GNR-CTAB diminished the cell viability about 47.0 ± 4.68 %, and no cells survived at a high dose of 200 μg/mL. In contrast to GNR-CTAB, folic acid modified GNR-MUA-PEI-FA caused no decrease on the cell viability at the concentration of 20 μg/mL, while retaining high viability (> 80 %) even at the high dose of 100 μg/mL (Figure 2B). Taken together, these data suggested FA significantly reduced cytotoxicity of GNRs.

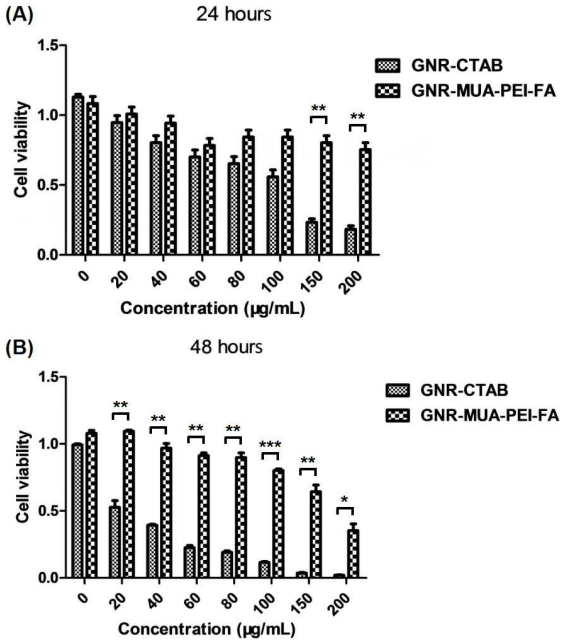

Figure 2. Assessment of cell viabilities. B16-BL6 cells were incubated with a medium containing different amount of GNR-CTAB or GNR-MUA-PEI-FA, and the final concentration of GNR-CTAB or GNR-MUA-PEI-FA was 0 μg/mL, 20 μg/mL, 40 μg/mL, 60 μg/mL, 80 μg/mL, 100 μg/mL, 150 μg/mL, and 200 μg/mL. After incubation for 24 hours (A) or 48 hours (B), the cell viabilities were measured by the MTT assay. (*, $P < 0.05$; **, $P < 0.01$; ***, $P < 0.001$)

3.3. Assessment of apoptosis.

To assess the capacity of causing apoptosis of GNR-CTAB and GNR-MUA-PEI-FA, we repeated above experiments by analyzing apoptosis of the B16-BL6 cells after incubation with various amounts of GNR-CTAB and GNR-MUA-PEI-FA, and then stained apoptotic cells with Annexin V-FITC/PI apoptosis detection kit and analyzed by flow cytometry (Figure 3). Compared to GNR-CTAB (Figure 3A and Figure 3C), GNR-MUA-PEI-FA (Figure 3B and Figure 3D) caused few cells to apoptosis even at high dose of 200 g/mL for 48 hours. These results suggested that when GNRs-CTAB had been modified with MUA-PEI-FA, GNR-MUA-PEI-FA had much lower cytotoxicity and better biocompatibility than GNRs-CTAB.

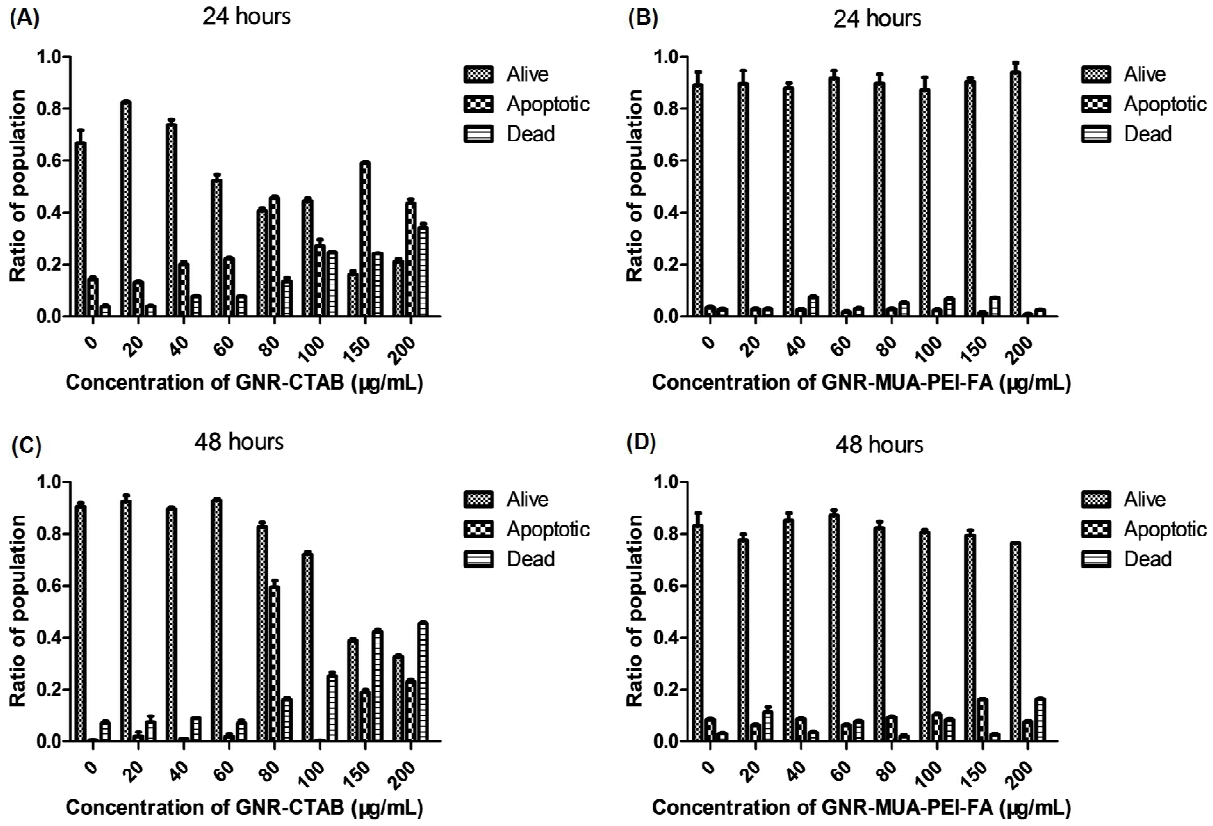

Figure 3. Apoptosis assay. The B16-BL6 cells were incubated with a series amount of GNR-CTAB (A and C) or GNR-MUA-PEI-FA (B and D) and t GNR-CTAB or GNR-MUA-PEI-FA at indicated concerntrations. After 24 hours (A and B) or 48 hours (C and D), the ratios of alive, apoptotic and dead cells were determined at 24

hours by Annexic V-FITC/PI Apoptosis Detection Kit and analyzed by flow cytometry. The Annexin V-FITC and PI both positive or only Annexin V-FITC positive cells were regarded as apoptotic; the only PI positive ones were calculated as dead; the double negative ones were alive. Error bars represent the standard deviation of 3 experiments.

3.4. Tumor-targeted delivery of siRNA.

One desirable function of nano-vectors is to condense DNA/RNA to form stable complexes against enzymatic degradation.[34] We thus tested the capacity of GNR-MUA-PEI-FA to condense siRNA electrostatically using a gel shift assay. In this assay, free siRNA migrates relatively unimpeded through the gel, while the migration of siRNA bound to GNR-MUA-PEI-FA is slowed down or stopped.[35] The result showed that, for GNR-MUA-PEI-FA, the ratio of GNR-MUA-PEI-FA:siRNA required to fully inhibit migration of siRNA was more than 8:1 (wt:wt) (Figure 4A). Therefore, when the ratio (wt:wt) of GNR-MUA-PEI-FA to siRNA is more than 8:1, GNR-MUA-PEI-FA could effectively adsorb all the siRNA molecules.

To assess the enhancement of cellular uptake due to folic acid, we compared the percentages of metastatic melanoma cell B16-BL6 which had up-taken Cy3-labelled siRNA (Cy3-siRNA) bound to different vehicles: GNR-MUA-PEI-FA and GNR-MUA-PEI *in vitro* for 4 hours. The transfection efficacy was determined by the Cy3 positive cells using flow cytometry. As shown in Figure 4B, GNR-MUA-PEI-FA achieved high transfection rate of 80.8 ± 0.50 %, which is similar to when using LIP2000 (a commercial standard siRNA transfection reagent) that showed 85.0 ± 1.60 % positively transfected cells. We also analyzed the influence of FA on the cellular uptake of GNRs and siRNA by B16-BL6 in Figure 4B. Compared to GNR-MUA-PEI-FA, GNR-MUA-PEI without FA dropped down the transfection rate to 42.4 ± 1.75 % (Figure 4B), which indicated FA could promote the cellular uptake of siRNA and GNRs by B16-BL6 significantly. Taken together, these results suggested that GNR-MUA-PEI-FA could be a comparative vehicle for siRNA transfecting B16-BL6, while FA is capable of enhancing cellular uptake of siRNA carried by GNRs.

Folic acid (FA, the synthetic form of folate) is a water-soluble B vitamin, which is essential for *de novo* synthesis and one carbon transfer reactions.[36] Folate receptors (FRs), also known as folate-binding proteins (FBP), are N-glycosylated proteins with high binding affinity to folate in vivo. Functional FR expression is low or absent in most non-malignant tissues, in contrast, neoplasias, especially epithelial carcinomas, consistently and uniformly express high levels of FRs.[36] The frequent overexpression within tumors and highly restricted distribution in normal tissues suggest that FRs can potentially be exploited as a tumor-specific cell surface marker that can be used in the targeted delivery of cancer therapeutics.[37] Since B16-F10 melanoma consistently express folate receptors,[38] it an ideal modal for investigating the potential therapeutic application of GNR-MUA-PEI-FA. Indeed, addition of folic acid (GNR-MUA-PEI-FA) significantly enhanced the siRNA delivery to

melanoma cell B16-BL6 (Figure 4B). To further confirm the tumor-specific targeting by FA, in a parallel experiment, we also performed quantitative measurements on the count of HUVEC as a non-tumor targeting experiments. We observed that as shown in Figure 4C, the correspondent percentages of HUVEC that had been transfected with Cy3-siRNA by GNR-MUA-PEI was 51.8 ± 2.75 %.The addition of folic acid using GNR-MUA-PEI-FA failed to increase transfection rate (47.8 ± 1.80 %) in HUVEC cells (Figure 4C), which was also much less than that observed in B16-BL6 (Figure 4B). These results suggested that folic acid is capable of facilitating GNR-MUA-PEI-FA targeting of melanoma cells (B16-BL6), and transfecting siRNA more efficiently in tumor cells than in vascular endothelial system cells (HUVEC). Thus, GNR-MUA-PEI-FA probably was an ideal carrier for delivery of siRNA to melanoma *in vivo*. Our results are in agreement with other studies, which have utilized gold nanorods for selective delivery of agents to cancer cells using enzyme activated release of payload selectively intracellularly.[39]

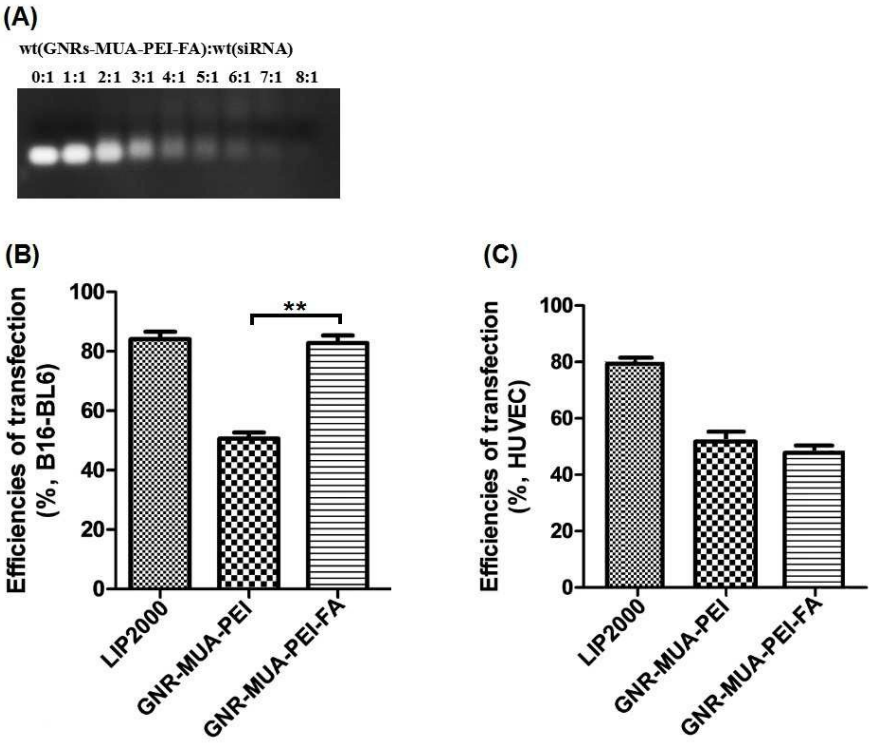

Figure 4. Tumor-targeted delivery of siRNA by GNR-MUA-PEI-FA. (A) Gel shift assay for assessing the siRNA-loading capacity of GNR-MUA-PEI-FA. Equal volumes containing 0.5 μg of siRNA and the desired amount of GNR-MUA-PEI-FA were mixed and incubated for 30 minutes at the indicated weight ratios of siRNA to GNR-MUA-PEI-FA. Electrophoresis was done and the gel was taken out for visualizing the bands. (B) Tumor-targeted delivery by GNR-MUA-PEI-FA. Cy3-GAPDH was used to assess the cellular uptake of LIP2000, GNR-MUA-PEI, GNR-MUA-PEI-FA as the vehicle for siRNA delivery. B16-BL6 (B) and HUVEC (C) were incubated with LIP2000/Cy3-GAPDH, GNR-MUA-PEI/Cy3-GAPDH, or GNR-MUA-PEI/Cy3-GAPDH-FA for 4 hours. The population of cell that had up-taken vehicle/Cy3-GAPDH

was determined by flow cytometry. Error bars represent the standard deviation of 3 experiments. (**, $P < 0.01$)

3.5. Validation of gene silencing by GNR-MUA-PEI/siRNA-FA.

Next, we attempted to validate the gene silencing ability of GNR-MUA-PEI/siRNA-FA, using the house-keeping gene Glyceraldehyde 3-phosphate dehydrogenase (GAPDH) as a reference and IDO2 as the siRNA target. After treatment with GNR-MUA-PEI-FA loading with IDO2 siRNA for 24 hours, relative siIDO2 mRNA levels were reduced by about 77.8 ± 3.72 % compared to the cells treated with a scrambled sequence non-targeting siRNA (siGL2) (Figure 5A). In Figure 5B and 5C, WB analysis was further confirmed that significant knockdown of IDO2 expression was successful after gene silencing. These results indicated that the siRNA could be released from GNR-MUA-PEI-FA and retain the biological functions of gene silencing. In support of this notion, Dzamukova et al created nanotube carriers with dextrin end stoppers to allow for selective intercellular release of encased payload.Specifically, the payload-filled nanotubes penetrate through the cellular membranes and intercellular glycosyl hydrolases-cause degradation of the dextrin tube-end stoppers triggers the release of the payload from inside the nanorod.[39] Future research may include incorporation of an enzyme-based activation of siRNA release using a nanoparticle delivery system and targeting enzymes associated with neoplasia.

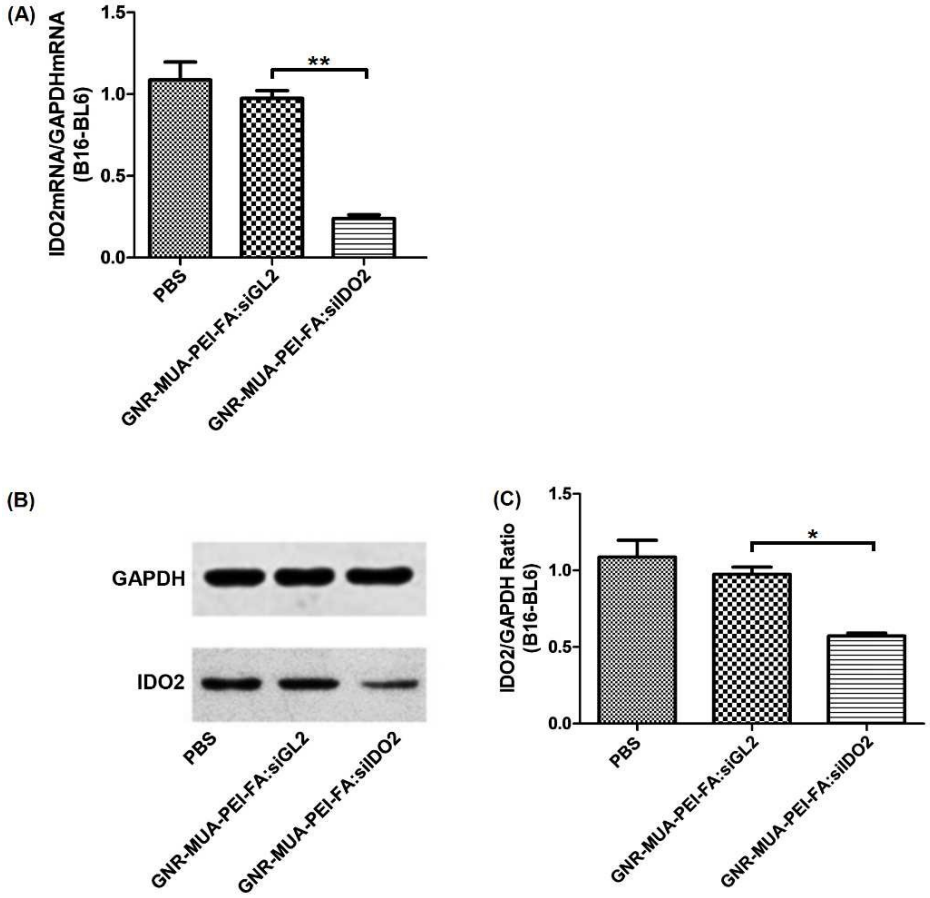

Figure 5. Gene silencing of GNR-MUA-PEI/siRNA-FA. (A) B16-BL6 cells were incubated with a final concentration of 16 μg/mL of GNR-MUA-PEI/siIDO2-FA (wt(GNR-MUA-PEI-FA):wt(siIDO2)=15:1) or GNR-MUA-PEI/siGL2-FA (wt(GNR-MUA-PEI-FA):wt(siGL2)=15:1) (as the non-specific siRNA control) or PBS for 24 hours, and then the mRNA expressions of IDO2 in the samples were quantified with qRT-PCR using GAPDH as a reference; (B) B16-BL6 cells were transfected with GNR-MUA-PEI/siIDO2-FA or GNR-MUA-PEI/siGL2-FA or PBS at the same concentrations as described above. 24 hours later, the amount of IDO2 or GAPDH was determined by western blot (WB) protein assays; (C) the calculation results of western blot of (B). Error bars represent the standard deviation of 3 experiments. (*, $P < 0.05$; **, $P < 0.01$)

3.6. Assessment of tumor-killing capacity of GNR-MUA-PEI-FA.

The photothermal therapeutic effects of GNR-MUA-PEI-FA in B16-BL6 cells was examined *in vitro* upon NIR laser irradiation. Tumor-killing of B16-BL6 cells was evaluated by MTT assay at 24 hours after incubating GNR-MUA-PEI-FA followed by laser irradiation. As shown in Figure 6A, when the power density of irradiation with 808 nm wavelength laser was 2 W/cm^2 for 0, 0.5, 1, 2, 5 and 10 minutes, initial tumor killing (19 %) of B16-BL6 cells by GNR-MUA-PEI-FA occurred as early as 1 minute of irradiation. The increased killing of tumor cells was observed, up to 57 %, 73 % and 73 %, when the laser irradiation time extended to 2, 5, and 10 minutes, respectively, as compared with control cells that received GNR-MUA-PEI-FA but without the dose of irradiation (Figure 6B). These results suggested that photothermal effects of GNRs using GNR-MUA-PEI-FA could be efficiently achieved to kill melanoma cells, and 5 minute irradiation showed an optimal killing capacity to tumor cells, therefore, which was applied for the next study.

We also measured the photothermal therapeutic effects of GNR-MUA-PEI-FA in B16-BL6 cells at different laser power density when the duration of irradiation was constant on 5 minutes (Figure 6B). The results suggested that 1 W/cm^2 is the minimum laser density necessary to kill tumor cells; when the laser power was added to 2 W/cm^2, killing of tumor cells by GNR-MUA-PEI-FA was significantly increased to 74 % (Figure 6B). An increase (95 %) of tumor cell killing by GNR-MUA-PEI-FA was observed when the laser power was set up at higher power (4 W/cm^2), however, control cells that was treated with PBS also induced up to 56 % cell death, suggesting the threshold of laser power should not exceed this maximum dose that may be harmful to the GNRs-untreated/normal cells in PTT. Thus the condition for the further *in vivo* experiments was optimized to be 1 w/cm^2 of the power density and 2 minutes of the irradiation duration, which could effectively achieve photothermal effects of GNRs without non-specific injury to the non-malignant control cells.

To investigate apoptosis of B16-BL6 induced by IDO2 knockdown, we carried out the comparison experiments of the treatments of GNR with or without presence of IDO2 siRNA . According to the flow cytometry results (Figure 6C(a, b, c)), the percentages of apoptotic cell population in the GNR-MUA-PEI/siIDO2-FA treated cells was 16.7 %, which was significantly higher than the cells treated with control GNR-MUA-PEI/siGL2-FA (6.2 %).

Addition of IDO2 siRNA remarkably increased tumor cells to apoptosis, which is also consistent to our earlier discovery of silencing IDO2 causing tumor cell apoptosis.[16] To clarify whether this increased apoptosis may enhance the killing ability of GNRs in PTT, we repeated above experiments under the condition of laser irradiation. As shown in Figure 6C(d, e, f), apoptosis (19.8 %) occurs in the GNR-MUA-PEI/siGL2-FA treatment along the combination of laser irradiation (808 nm, 2 w/cm^2, 5 minutes), while GNR-MUA-PEI/siIDO2-FA, which incorporated with IDO2 siRNA, dramatically increased tumor cell apoptosis to 26.9 %. These data suggested that IDO2 knockdown by GNR-MUA-PEI/siIDO2-FA induces tumor B16-BL6 cells to apoptosis and enhances the tumor cell killing ability of photothermal effects of GNRs, highlighting that GNR-MUA-PEI/siIDO2-FA could exert synergy of photothermal effects of GNRs and the IDO2 knockdown inducing tumor cell apoptosis.

In our studies the use of gold nanoparticles to deliver immune stimulatory siRNA, while concurrently inducing killing of cancer cells via laser induced hyperthermia was accomplished. A similar approach to ours was developed by Chen et al,[40] who utilized gold nanoparticles generated in a multi-layered manner by stabilization with hexadecyltrimethylammonium bromide and layering with polyelectrolytes and BSA. This approach was developed for selective release of doxorubicin subsequent to photothermal activation. Comparison between this approach and the approach developed by us for delivery of siRNA will require experimentation.

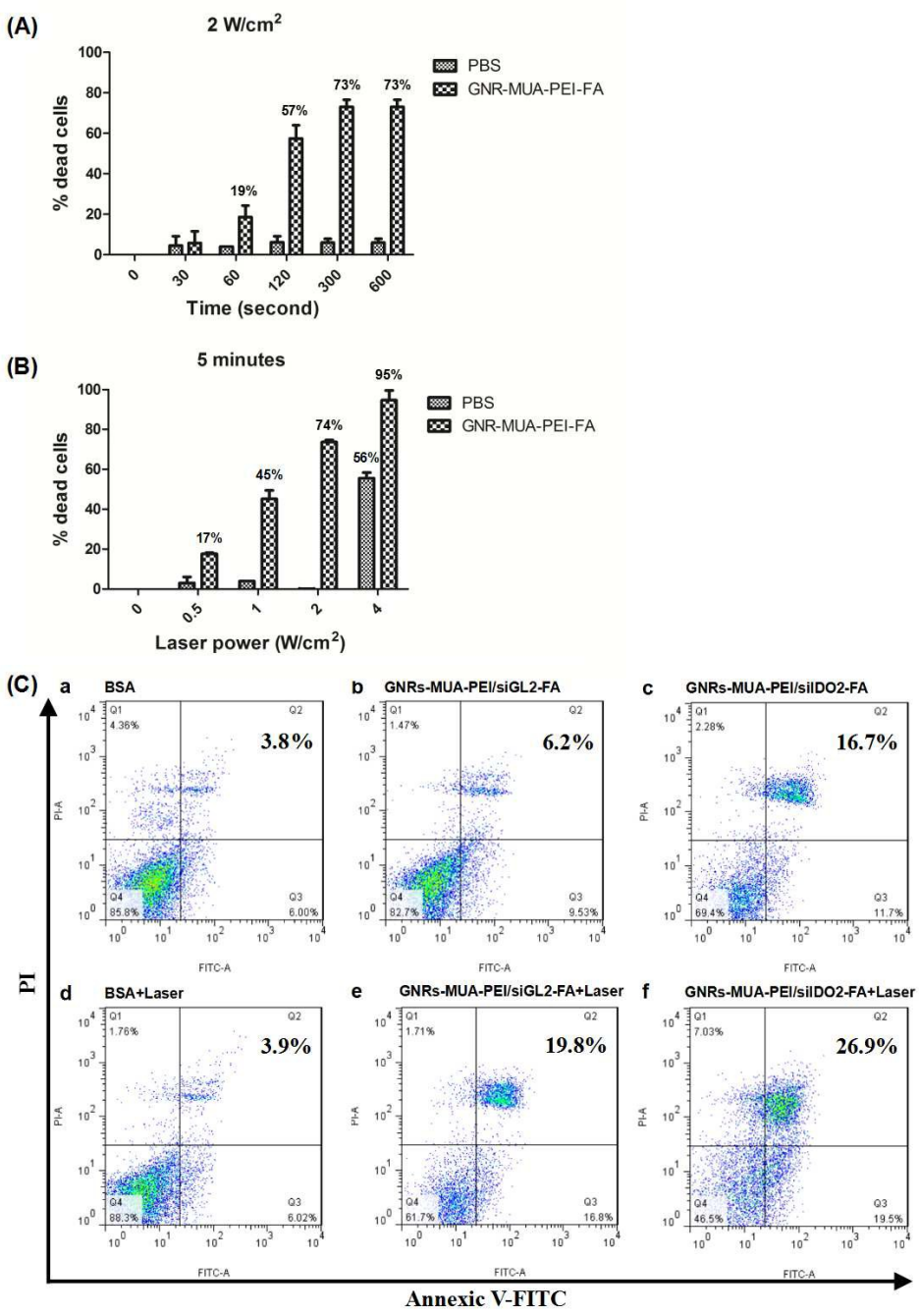

Figure 6. ***In vitro*** **photothermal effects of GNR-MUA-PEI-FA and GNR-MUA-PEI/siIDO2-FA.** B16-BL6 cells were incubated with a final concentration of 15 μg/mL of GNR-MUA-PEI-FA or PBS for overnight. Subsequently, the cells were irradiated at (A) 2 W/cm^2 for various times (0 minutes, 0.5 minutes, 1 minutes, 2 minutes, 5 minutes, 10 minutes) or at (B) 5 minutes for different power density (0 W/cm^2, 0.5 W/cm^2, 1 W/cm^2, 2 W/cm^2, 4 W/cm^2). After 24 hours, the cell viabilities were measured by the MTT assay and the percentages of dead cells = (cell viabilities before laser irradiation - cell viabilities after laser irradiation) / (cell viabilities before laser irradiation). (C) Apoptosis of tumor cells induced by GNR-MUA-PEI/siIDO2-FA. B16-BL6 cells were incubated with PBS (a) or GNR-MUA-PEI/siGL2-FA (b), or GNR-MUA-PEI-FA-siIDO2 (c), at the final

concentration of 16 μg/mL of wt(GNR-MUA-PEI-FA):wt(siIDO2) =15:1) for overnight. Cells were remained no irradiation (a, b, c) or were irradiated (d, e, f) at 2 W/cm^2 for 5 minutes with the wavelength of laser was 808 nm. The apoptotic and necrotic cell populations were determined at 24 hours by Annexic V-FITC/PI Apoptosis Detection Kit and analyzed by flow cytometry. Error bars represent the standard deviation of 3 experiments.

3.7. Transdermal delivery of siRNA to melanoma by GNR-MUA-PEI-FA.

Cutaneous melanoma is a highly invasive disease. It would be ideal if there were a topical drug delivery system to suppress the growth of melanoma or even induce tumor regression in the case of immediate surgical removal is not possible. Therefore, we next explored the *in vivo* transdermal delivery of siRNA to melanoma by GNR-MUA-PEI-FA. The tumors were generated by subcutaneous injection of B6-BL6 cells on the back of C57BL/6 mice. After two weeks, the H&E staining histological section evidenced that the melanoma models were successfully prepared (Figure 8A). Mixtures of Cy3-labeled siGAPDH, GNR-MUA-PEI/Cy3-labeled siGAPDH or GNR-MUA-PEI/Cy3-labeled siGAPDH-FA with glycerin and DMSO were topically applied on the skins above the inoculated tumors for 4 hours before analysis of fluorescent microscopy images of melanoma tissues (Figure 7). The Cy3-labeled siGAPDH siRNA alone was not able to enter the cells and showed almost no fluorescence (Figure 7A and 7B), while siRNA delivered by GNR-MUA-PEI only showed light fluorescence (Figure 7C and 7D). In contrast, targeted delivery of siRNA using GNR-MUA-PEI-FA displayed the most intense fluorescence (Figure 7E and 7F), suggesting that GNR-MUA-PEI-FA is as an effective transdermal reagent to reach the melanoma tissue for delivering siRNA to melanoma and promoting the cellular uptake of GNR-MUA-PEI-FA/siRNA by the melanoma cells *in vivo*.

Nevertheless, the clinical development of the current approach will need to take into consideration the shape of the nanoparticle. As reviewed by Troung et al, shape influences biodistribution, selective uptake into cells, as well as possible selectivity of tumor uptake versus uptake into the tumor microenvironment. While advantages of nanorods to other shapes have been previously demonstrated in the cited review,[20] future optimization studies will explore this questions.

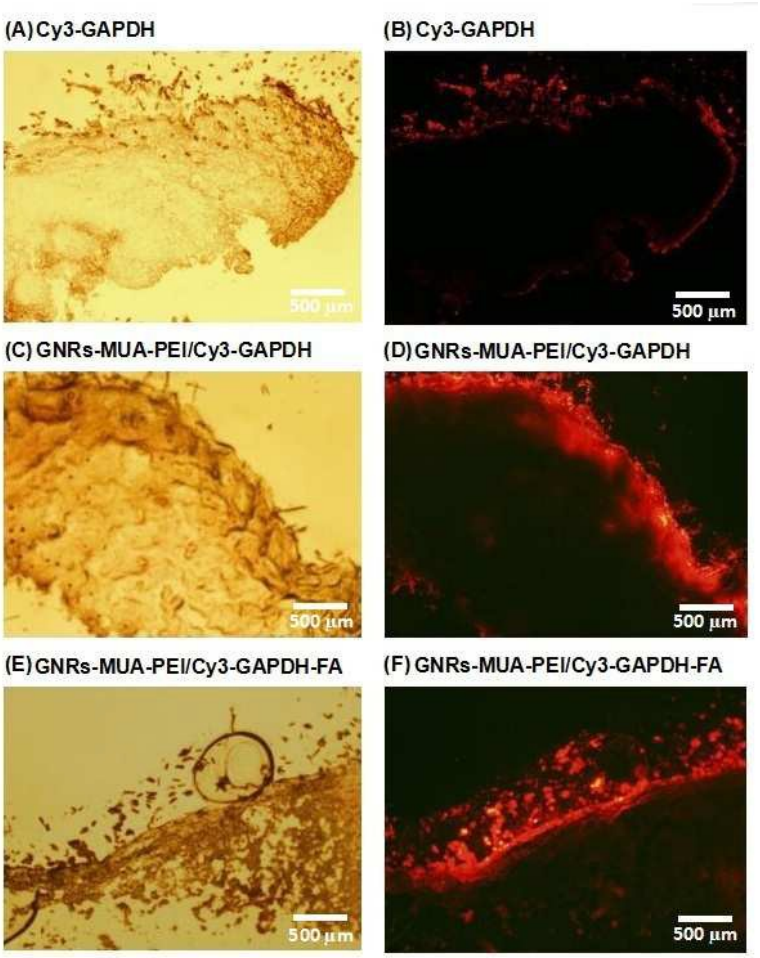

Figure 7. ***In vivo*** **topical tumor-specific delivery of siRNA by GNR-MUA-PEI-FA.** B16-BL6 melanoma tumor cells were inoculated on to C57BL/6 mice as described in Materials and Methods. After 2 weeks, mice were anesthetized and the following reagents were applied on the skins above inoculated tumors: (A) and (B) Cy3-siGAPDH, (C) and (D) GNR-MUA-PEI/Cy3-siGAPDH, and (E) and (F) GNR-MUA-PEI/Cy3-siGAPDH-FA (all containing 6 μg of Cy3-siRNA, wt(GNR-MUA-PEI or GNR-MUA-PEI-FA):wt(Cy3-siRNA)=15:1). 4 hours after above topical application of Cy3-labbeled siRNA, and then the mice were scarified and the tumors were collected. The tumors tissues were frozen sectioned and the images were visualized with a fluorescence microscope.

3.8. Evaluation of anti-tumor efficacy of GNR-MUA-PEI/siIDO2-FA in photothermal therapy (PTT).

To investigate the *in vivo* anti-tumor efficacy of GNR-MUA-PEI/siIDO2-FA, which initiated a PTT of GNRs by NIR laser and enhanced anti-tumor therapy due to silencing IDO2, we tested therapeutic PTT in melanoma bearing mice. After 14 day treatment of melanoma in Figure 8B, compared to PBS treating melanoma, GNR-MUA-PEI/siGL2-FA did not inhibit the tumor growth without the laser irradiation. In contrast, treatment of GNR-MUA-PEI/siGL2-FA with the laser irradiation (808 nm, 1 W/cm^2, 2 minutes)

significantly decreased the tumor volume (Figure 8B), demonstrating the photothermal effects of GNRs. In addition, the treatment of GNR-MUA-PEI/siIDO2-FA, in combination of irradiation, showed the best therapeutic effects, implying the critical role of silencing IDO2 in inhibiting the tumor growth more effectively. In addition, after 14 day treatment of melanoma, the mice were sacrificed and the tumors were collected at the end point of observation. The size (Figure 8C) and weight (Figure 8D) of tumors were confirmed the PTT enhanced by silencing IDO2 as a promising treatment strategy for melanoma therapy using GNR-MUA-PEI/siIDO2-FA. Taken together, these data are the first demonstration that the enhanced anti-tumor therapy is achievable by knocking down IDO2 together with the photothermal effects of GNRs in melanoma therapy.

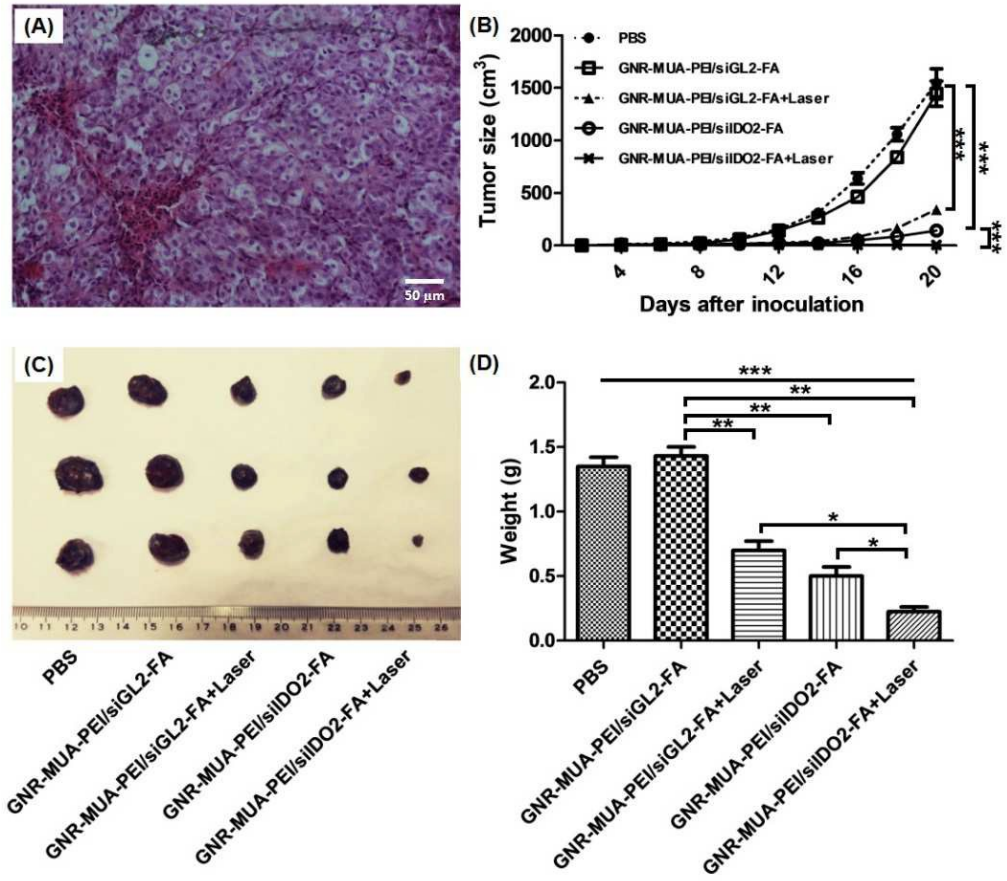

Figure 8. ***In vivo*** **photothermal effects of GNR-MUA-PEI/siIDO2-FA for melanoma.** (A) Melanoma models and histology sections. Female C57BL/6 mice were inoculated with B16-BL6 cells. After 2 weeks, mice were scarified. The tumors were collected and the hematoxylin and eosin (HE) staining was performed on paraffin-embedded sections. The prepared specimen was examined using a light microscope. Melanoma bearing mice were treated with PBS or GNR-MUA-PEI-FA/siRNA (wt(GNR-MUA-PEI-FA):wt(siRNA)=15:1, 6 μg, siIDO2 or siScrambled), by a topical application onto the skins above the tumors on day 6, 10, 14, 18. Twelve hours after each application of above mixture, a laser irradiation (1 W/cm^2, 2 minutes) was conducted. The tumor sizes of growth were measured with caliper (B). 20 days after tumor inoculation, the mice were sacrificed

and tumors were collected. The images of tumor were displayed (C) and the tumor weights were measured (D). Error bars represent the standard deviation of 3 experiments. (*, $P < 0.05$; **, $P < 0.01$; ***, $P < 0.001$).

4. Conclusion

In summary, we have designed and generated a novel nanoplatform GNR-MUA-PEI-FA/siIDO2, which possesses several integrated components: GNRs that exerts photothermal killing of melanoma cells upon NIR laser, FA that promotes tumor-specific delivery of siRNA to melanoma cells, and siIDO2 that can enhance inhibition of tumor growth upon knockdown of IDO2 gene. This new nanoplatform of GNR-MUA-PEI/siIDO2-FA represents a novel concept of GNR-based photothermal therapy and enhanced anti-tumor therapy by silencing IDO2 on the tumor cells. Encouragingly, this GNR-MUA-PEI/siIDO2-FA nanoplatform has displayed multiple advantages such as low cytotoxicity and improved biocompatibility, tumor specific targeting ability into B16-BL6 cells, and efficient induction of gene silencing. The feasibility of this new methods was evidenced by a robust therapeutic efficacy by inhibiting the growth of tumors in a murine melanoma model at a low laser power density (1 W/cm^2, 2 minutes), which paves a novel way for cancer therapy by combining photothermia and gene silencing of IDO2.

Acknowledgments

This study was supported by grants from Natural Science Foundation of China (NSFC, No. 81273303, 11574255), Jiangxi Provincial Natural Science Foundation (20151BAB205060, 20124ACB00800, 20133BBG70019), Nanchang University Doctoral Foundation (No. 06301097), Jiangxi Provincial Post-Doctoral Foundation (No. 00018422), and Fujian Provincial Science and Technology Plan (Cooperation) Key Project (No. 2014I0016).

Author Contributions

All the authors are contributed to this manuscript. Planned experiments: Y.Z., W.M.; Performed experiments Y.Z., N.S., J.F., Y.L., X.Z., S.P., Z.Y., Y.G., Z.W.; Analyzed data: Y.Z., W.M., Q.S., Y.F., K.Y., N.Z.; Wrote the paper: Y.Z., N.S., T.E.I, W.M. All authors are assured that we met the criteria for authorship and all reviewed the manuscript.

Disclosure: Conflict of Interest

The authors of this manuscript have no conflicts of interest to disclose.

References

1 I. Russo, F. Caroppo and M. Alaibac, *Cancers*, 2015, **7**, 1371-1387.

2 A. M. Eggermont, A. Spatz and C. Robert, *Lancet*, 2014, **383**, 816-827.

3 National Cancer Institute. *Surveillance, Epidemiology and End Results*. http://www.seer.cancer.gov/statfacts/ (accessed June 30, 2013).

4 M. R. Middleton, P. Lorigan, J. Owen, L. Ashcroft, S. M. Lee, P. Harper and N. Thatcher, *Br. J. Cancer*, 2000, **82**, 1158-1162.

5 A. A. Tarhini, J. M. Kirkwood, W. E. Gooding, S. Moschos and S. S. Agarwala, *Cancer*, 2008, **113**, 1632-1640.

6 M. Singh and W. W. Overwijk, *Cancer Immunol. Immunother.*, 2015, **64**, 911-921.

7 M. Terabe and J. A. Berzofsky, *Trends Immunol.*, 2007, **28**, 491-496.

8 D. H. Munn, *Curr. Opin. Immunol.*, 2006, **18**, 220-225.

9 J. B. Katz, A. J. Muller and G. C. Prendergast, *Immunol. Rev.*, 2008, **222**, 206-221.

10 Y. Yan, G. X. Zhang, B. Gran, F. Fallarino, S. Yu, H. Li, M. L. Cullimore, A. Rostami and H. Xu, *J. Immunol.*, 2010, **185**, 5953-5961.

11 H. J. Ball, A. Sanchez-Perez, S. Weiser, C. J. Austin, F. Astelbauer, J. Miu, J. A. McQuillan, R. Stocker, L. S. Jermiin and N. H. Hunt, *Gene*, 2007, **396**, 203-213.

12 X. Zheng, J. Koropatnick, M. Li, X. Zhang, F. Ling, X. Ren, X. Hao, H. Sun, C. Vladau, J. A. Franek, B. Feng, B. L. Urquhart, R. Zhong, D. J. Freeman, B. Garcia and W. P. Min, *J. Immunol.*, 2006, **177**, 5639-5646.

13 C. A. Blache, E. R. Manuel, T. I. Kaltcheva, A. N. Wong, J. D. Ellenhorn, B. R. Blazar and D. J. Diamond, *Cancer Res.*, 2012, **72**, 6447-6456.

14 X. Zheng, J. Koropatnick, D. Chen, T. Velenosi, H. Ling, X. Zhang, N. Jiang, B. Navarro, T. E. Ichim, B. Urquhart and W. Min, *Int. J. Cancer*, 2013, **132**, 967-977.

15 S. Maleki Vareki, D. Chen, C. Di Cresce, P. J. Ferguson, R. Figueredo, M. Pampillo, M. Rytelewski, M. Vincent, W. Min, X. Zheng and J. Koropatnick, *PloS One*, 2015, **10**, e0143435.

16 Y. Liu, Y. Zhang, X. Zheng, X. Zhang, H. Wang, Q. Li, K. Yuan, N. Zhou, Y. Yu, N. Song, J. Fu and W. Min, *Oncotarget*, 2016, DOI: 10.18632/oncotarget.8617.

17 A. Fire, S. Xu, M. K. Montgomery, S. A. Kostas, S. E. Driver and C. C. Mello, *Nature*, 1998, **391**, 806-811.

18 H. Borna, S. Imani, M. Iman and S. Azimzadeh Jamalkandi, *Expert Opin. Biol. Ther.*, 2015, **15**, 269-285.

19 D. D. Lasic and D. Papahajopoulos, *Science*, 1995, **267**, 1275

20 N. P. Truong, M. R. Whittaker, C. W. Mak, and T. P. Davis, *Expert Opin. Drug Deliv.*, 2015, **12**, 129-142.

21 T. Lammers, F. Kiessling and W. E. Hennink, *J. Control. Release*, 2012, **161**, 175-187.

22 S. Venkataraman, J. L. Hedrick, Z. Y. Ong, C. Yang, P. L. Ee, P. T. Hammond and Y. Y. Yang, *Adv. Drug Deliv. Rev.*, 2011, **63**, 1228.

23 X. Hu, J. Hu, J. Tian, Z. Ge, G. Zhang, K. Luo and S. Liu, *J. Am. Chem. Soc.*, 2013, **135**, 17617

24 P. Wagstaff, A. Ingels, P. Zondervan, J. J. de la Rosette and M. P. Laguna, *Curr. Opin. Urol.*, 2014, **24**, 474-482.

25 T. J. Vogl, P. Farshid, N. N. Naguib and S. Zangos, *Eur. Radiol.*, 2013, **23**, 797-804.

26 A. Poletti, G. Fracasso, G. Conti, R. Pilot and V. Amendola, *Nanoscale*, 2015, **7**, 13702-13714.

27 J. Song, P. Huang, H. Duan and X. Chen, *Acc. Chem. Res.*, 2015, **48**, 2506-2515.

28 R. K. Kannadorai, G. G. Chiew, K. Q. Luo and Q. Liu, *Cancer Lett.*, 2015, **357**, 152-159.

29 J. Song, L. Pu, J. Zhou, B. Duan and H. Duan, *ACS nano*, 2013, **7**, 9947-9960.

30 Z. Chen, X. Shan, Y. Guan, S. Wang, J. J. Zhu and N. Tao, *ACS Nano*, 2015, **9**, 11574-11581.

31 A. Heber, M. Selmke and F. Cichos, *Phys. Chem. Chem. Phys.*, 2015, **17**, 20868-20872.

32 B. Nikoobakht, M. A. El-Sayed, *Chem. Mater,* 2003, **15**, 1957-62.

33 E. J. Jin, Y. A. Choi, J. K. Sonn and S. S. Kang, *Mol. Cells*, 2007, **24**, 139-147.

34 D. Putnam, *Nat. Mater.*, 2006, **5**, 439-451.

35 K. S. Siu, D. Chen, X. Zheng, X. Zhang, N. Johnston, Y. Liu, K. Yuan, J. Koropatnick, E. R. Gillies and W. P. Min, *Biomaterials*, 2014, **35**, 3435-3442.

36 X. Pan and R. J. Lee, *Expert Opin. Drug Deliv.*, 2004, **1**, 7-17.

37 J. Sudimack and R. J. Lee, *Adv. Drug Deliv. Rev.*, 2000, **41**, 147-162.

38 T. Kurosaki, T. Morishita, Y. Kodama, K. Sato, H. Nakagawa, N. Higuchi, T. Nakamura, T. Hamamoto, H. Sasaki and T. Kitahara, *Mol. Pharm.*, 2011, **8**, 913-919.

39 M. R. Dzamukova, E. A. Naumenko, Y. M. Lvov, and R. F. Fakhrullin, *Sci. Rep.*, 2015, **5**, 10560.

40 H. Chen, X. Chi, B. Li, M. Zhang, Y. Ma, S. Achilefu and Y. Gu, *Biomater. Sci*., 2014, **2**,996-1006.